

Nanoscale

Accepted Manuscript



This is an *Accepted Manuscript*, which has been through the Royal Society of Chemistry peer review process and has been accepted for publication.

Accepted Manuscripts are published online shortly after acceptance, before technical editing, formatting and proof reading. Using this free service, authors can make their results available to the community, in citable form, before we publish the edited article. We will replace this *Accepted Manuscript* with the edited and formatted *Advance Article* as soon as it is available.

You can find more information about *Accepted Manuscripts* in the [Information for Authors](#).

Please note that technical editing may introduce minor changes to the text and/or graphics, which may alter content. The journal's standard [Terms & Conditions](#) and the [Ethical guidelines](#) still apply. In no event shall the Royal Society of Chemistry be held responsible for any errors or omissions in this *Accepted Manuscript* or any consequences arising from the use of any information it contains.

ARTICLE

Induction of Apoptosis in Human Cancer Cells by Targeting Mitochondria with Gold Nanoparticles

Cite this: DOI: 10.1039/x0xx00000x

M. M. Mkandawire,^{a,b,c} M. Lakatos,^c A. Springer,^c A. Clemens,^b D. Appelhans,^d U. Krause-Buchholz,^b W. Pompe,^b G. Rödel^b and M. Mkandawire,^{c,e}

Received 00th January 2012,

Accepted 00th January 2012

DOI: 10.1039/x0xx00000x

www.rsc.org/

A major challenge in designing cancer therapies is inducing cancer cell apoptosis, although activation of intrinsic apoptotic pathways by targeting gold nanoparticles to mitochondria is promising. We report an *in vitro* procedure targeting mitochondria with conjugated gold nanoparticles and investigating effects on apoptosis induction in the human breast cancer cell line Jimt-1. Gold nanoparticles were conjugated to a variant of turbo green fluorescent protein (mitoTGFP) harbouring an amino-terminal mitochondrial localization signal. Au nanoparticle conjugates were further complexed with cationic maltotriose-modified poly(propylene imine) third generation dendrimers. Fluorescence and transmission electron microscopy revealed that Au nanoparticle conjugates were directed to mitochondria upon transfection, causing partial rupture of the outer mitochondrial membrane triggering cell death. The ability to target Au nanoparticles into mitochondria of breast cancer cells and induce apoptosis reveals an alternative application of Au nanoparticles in photothermal therapy of cancer.

Introduction

One mechanism for therapeutic destruction of cancer cells is to induce apoptosis either extrinsically by targeting cell surface receptors, or intrinsically via mitochondria.¹ In the extrinsic route, activated cell death receptors lead to activation of caspase 8, which results in a caspase-signalling cascade. In the mitochondria-mediated pathway, the formation of a multimeric Apaf-1/cytochrome *c* complex initiates activation of procaspase 9, which cleaves and triggers downstream caspase 3, 6, and 7.² Consequently, mitochondria are an attractive target for the design of effective, specific cancer therapeutics resulting in less collateral damage to surrounding non-cancerous cells.^{3, 4} A current strategy being investigated is exploiting photothermal effect of gold nanoparticles (AuNPs) in the presence of low energy sources to induce extrinsic or mitochondrial-mediated apoptosis.⁵⁻⁸

AuNPs have shown immense potential for cancer diagnosis and therapy based on their surface plasmon resonance (SPR) enhanced light scattering and absorption.^{9, 10} AuNPs efficiently convert absorbed light into localized heat, which can be exploited for selective laser photothermal therapies for cancer.⁵ Additionally, conjugation of AuNPs to ligands specifically targeting biomarkers on cancer cells allows imaging and detection as well as photothermal treatment.^{6, 7, 11} Several studies have documented intracellular delivery and internalization of AuNPs including their incorporation into

mitochondria to induce apoptosis.^{3, 8, 12} However, targeting intracellular organelles in living cells remains a challenge due to the aggregation behaviour of AuNPs and their inefficient release from endosomes.

To circumvent this problem, we explored the use of cationic maltotriose-modified poly(propylene imine) (PPI) dendrimers as transfection reagents of AuNPs into Jimt-1 cells. The resulting AuNP-protein and dendrimer complexes are considered dendriplexes. Glycosylated dendrimers and hyperbranched polymers possess high transfection efficiency and biocompatible properties.¹³⁻¹⁵ For efficient delivery to target organelles, escape of polyplexes (complexes between oligo/polynucleic acids and cationic polymeric materials),¹⁶ from the endosomes is a prerequisite.⁴ The polyplexes are known to exit endosomes via the “proton-sponge” mechanism.¹³ Furthermore, cationic open shell and neutral dense shell PPI glycodendrimers can be used as transfection and stabilization agents for various particles¹⁷⁻¹⁹ and as biological agents to interfere with fibril assemblies of prion peptides²⁰ and proteins.²¹ Other well-established cationic carrier systems such as liposomes and the cell penetrating peptide protamine have been shown to be unsuitable for transfection of green diamond-antibody conjugates to the cytoplasm.¹⁶ However, open and dense maltotriose shell PPI glycodendrimers possess promisingly low or no toxicity under *in vivo* conditions.²² Motivated by the fact that this glycodendrimer has some advantages for stabilizing and

internalizing anionic hybrid conjugates in comparison to other carrier systems, in this study we also used the cationic 3rd generation PPI glycodendrimer with open maltotriose shell (PPI-Mal-III G3)¹⁸ for transfection of AuNP conjugates.

The aim of our study was to investigate selective targeting of AuNPs to mitochondria of Jimt-1 cancer cells to initiate apoptotic pathways. Jimt-1 cells are resistant to trastuzumab, a cancer drug, which targets cell surface receptors to induce apoptosis.²³ To target AuNPs to mitochondria and to follow their intracellular delivery, we conjugated AuNPs with green fluorescent protein harbouring the mitochondrial (mt) localization sequence of the inner membrane protein Cox8 at its amino terminus (mitoTGFP). In previous studies, the successful delivery of ultra-small AuNPs (2.7 nm diameter) conjugated to doxorubicin into the cell nuclei with DNA damage the likely cause of induced apoptosis.⁸ Another study demonstrated that Au nanorods (length 55.6 ± 7.8 nm, width 13.3 ± 1.8 nm) could be intracellularly directed to mitochondria in cancer cells, but not in mesenchymal cells, although the uptake pathways in both cell types were similar.²⁴

Results and discussion

Characteristics of AuNP conjugates

To explore the cellular uptake and intracellular trafficking of the mitoTGFP-AuNP conjugates stabilized by glycodendrimer PPI-Mal-III G3, we used citrate-stabilized AuNPs (20 nm) for TEM visualization. AuNPs were synthesized according to Frens et al.²⁵, and characterized by TEM (supporting information) and UV-Vis spectroscopy (figure 1a). Conjugation of mitoTGFP to AuNPs is by non-covalent binding of the protein to AuNPs at pH values close to the isoelectric point of the protein, in the case eGFP at pH 5.5 as described previously^{7,26}. Bioconjugates were analysed by optical changes in UV-Vis absorbance spectra due to the plasmon resonance of AuNPs.^{7,27} Adsorption of PEG to AuNPs showed a 6 nm red shift of the plasmon peak (figure 1). Upon conjugation of AuNPs to mitoTGFP and HAeGFP, a 12 nm red shift was observed, denoting successful conjugation along with a damping of the plasmon resonance band indicating molecule attachment on the particle surface (figure 1). Variation in red shift is dependent on differences in the dielectric nature of the nanoparticle medium,²⁸ as such, PEG-AuNPs show a much smaller red shift than either mitoTGFP- or HAeGFP-AuNPs.

To confirm the conjugation, 40 μ l of mitoTGFP-AuNP and HAeGFP-AuNP conjugates were loaded on a 0.5% agarose gel as described in Materials and Methods. Migration towards the cathode confirms the net negative charge of the conjugates in TBE buffer (pH 8.0). The net negative charge originated from the proteins mitoTGFP and HAeGFP with pI values of 5.8 and 5.9, respectively. Previous studies found the red shift of AuNPs conjugated to Ribonuclease S was dependent on the size and the amount of adsorbate AuNP.²⁹

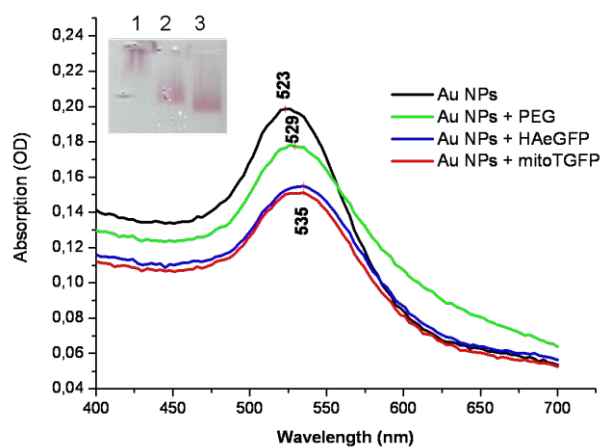


Figure 1. Absorption spectrum of 20 nm diameter AuNPs showing a 6 nm red shift in the plasmon resonance peak upon conjugation of the AuNPs to the polymer PEG, and a 12 nm red shift to the proteins. Insert are runs of 40 μ l AuNP conjugate on 0.5% agarose gel at 10 kV per cm to confirm the conjugation: (see insert). Lane 1 depicts AuNPs conjugated to PEG; lane 2 depicts AuNPs conjugated to HAeGFP; and, lane 3 is for AuNPs conjugated to mitoTGFP. Due to the differences in electronegativity of the proteins, mitoTGFP-AuNPs migrated faster than HAeGFP-AuNPs.

Transfection of AuNP conjugates

Conjugate uptake into cells requires a transfection reagent such as sugar-decorated dendritic glycopolymers.^{13, 14, 17, 30} In this study, we used cationic PPI-Mal-III G3 to mediate transfection of anionic protein-AuNP complexes into Jimt-1 cells; to demonstrate effectiveness of PPI-Mal-III G3 as a transfection reagent, mitoTGFP-AuNP conjugates were transfected either in the presence or absence of dendrimers. One hour after stopping transfection, cells were fixed and prepared for TEM. No evidence of mitoTGFP-AuNPs inside cells was obtained in the absence of PPI-Mal-III G3 (figure 2 (a)). In contrast, TEM micrographs of cells transfected with mitoTGFP-AuNP conjugates in the presence of PPI-Mal-III G3 revealed AuNPs as black spots inside cells (figures 2 (b) and (c)), confirming PPI-Mal-III G3 can mediate transfection of AuNP conjugates. Receptor-mediated endocytosis is the most likely uptake route of the dendrimer-protein AuNP complex due to oligosaccharide groups on the dendrimer AuNP.¹³

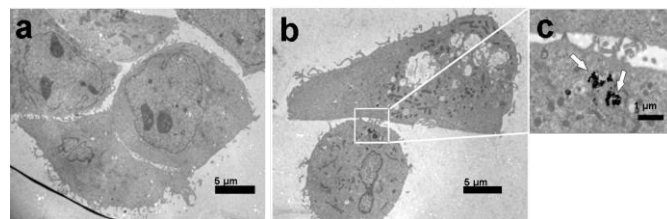


Figure 2. (a) TEM micrographs of breast cancer cells incubated with mitoTGFP-AuNPs in the absence of PPI-Mal-III G3 and in (b) in the presence of the glycodendrimer. In both cases, cells were fixed 1 hour after stopping transfection. In (c) a magnified TEM micrograph of the part shown in (b) depicts AuNPs as black spots or clusters (see arrows) inside cells. Scale bars are 5 μ m for (a) and (b) and 1 μ m for (c).

Next, we investigated targeting of AuNP conjugates using cells transfected with PEG-AuNPs, HAeGFP-AuNPs, and mitoTGFP-AuNPs. After transfection, cells were incubated in serum-containing medium for 24 h to permit targeting of AuNPs conjugates to intracellular organelles. TEM micrographs of cells transfected with PEG-AuNPs showed AuNPs as black spots in endosomes (figure 3 (a)) as they have previously been reported³¹ and as we similarly found for HAeGFP-AuNPs (figure 3 (b)). Several studies have reported the uptake and intracellular trafficking of protein-coated nanoparticles^{32, 33} such as ligand-conjugated quantum dots, which generally followed the same uptake pathway as ligands, but with conjugates arrested in endosomes.³² In our experiments, HAeGFP AuNPs also accumulated in endosomes and partly in lysosomes (figure 3(b)) suggesting an endo-/lysosomal pathway. In contrast, transfections with mitoTGFP-AuNPs demonstrated that nanoparticles are partially targeted to the inner mitochondrial membrane (figure 3 (c)). Previously, conjugation of organelle-specific targeting sequences to quantum dots resulted in delivery to either the nucleus or mitochondria.³⁴ The different fates of AuNP conjugates confirms previous observations that surface ligands play an important role in intracellular trafficking of nanoparticles.³⁵ We also observed different uptake mechanisms (See supplementary figure S1), which are known to result in different downstream intracellular trafficking.³⁶ An obvious explanation would be that the dendrimers target the NP to mitochondria (the electronegative pole within a eukaryotic cell) due to their cationic nature. However, our data on targeting of HA-eGFP do not support this view. Hence, we assume that the dendrimer coatings of the MitoTGFP-AuNP conjugates are removed during intracellular trafficking, thus exposing the mt targeting sequence of MitoTGFP-AuNP.

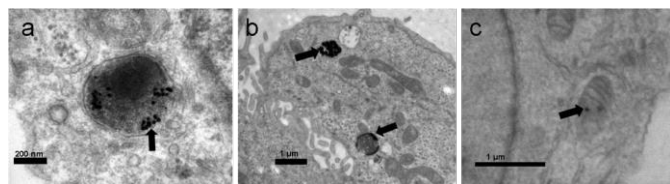


Figure 3. (a) TEM micrographs of breast cancer cells transfected with PEG-AuNPs (20 nm). Black spots representing AuNPs were observed in endosomes (see arrow). (b) TEM micrograph of AuNPs in early endosomes (upper arrow) and lysosomes (lower arrow) in cells that were transfected with AuNPs conjugated to HAeGFP. In (c) AuNPs conjugated to mitoTGFP associate with mitochondria. Scale bars are 200 nm for a, and 1 μ m for b and c.

MitoTGFP-AuNPs, transfected by PPI-Mal-III G3, enter the cells, early endosomes, cytosol, and mitochondria, and they are finally localized in the inner mitochondrial membrane (figure 4) suggesting at least some mitoTGFP-AuNPs evade the lysosomal pathway. After uptake, mitoTGFP-AuNPs are enclosed in early endosomes (figure 4(a)), which eventually rupture thereby releasing mitoTGFP-AuNPs to the cytosol (figure 4 (b)). Due to the mitochondrial-targeting signal, mitoTGFP-AuNPs are directed to mitochondria and pass through the outer mitochondrial membrane (OMM) (figure 4

(c)). Although how AuNP conjugates target mitochondria is not clear, most likely cytosolic factors such as mitochondrial import stimulating factor (MSF) play an important role AuNP.^{37, 38} MitoTGFP-AuNPs probably follow the uptake mechanism of Cox8, which is mediated by two translocase protein complexes of the outer and inner mitochondrial membranes.³⁹ However, the size of the import pore (<2.6 nm) on inner and out mitochondrial membranes could block the entrance of larger nanoparticles⁴⁰ although in our case, it is likely AuNP complexes (~ 20 nm) partially rupture OMM upon entry (as seen in TEM micrographs), where mitoTGFP-AuNPs co-localize with the inner mt membrane (figures 4 (c) and 3(c)).

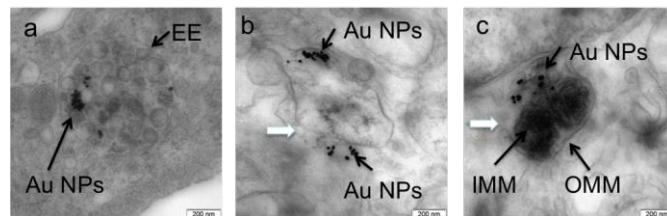


Figure 4. TEM micrographs of breast cancer cells transfected with mitoTGFP-AuNPs in the presence of maltotriose-modified PPI dendrimers showing intracellular trafficking pathway of mitoTGFP-AuNPs. In (a) mitoTGFP-AuNPs are contained in an early endosome (EE); in (b) shows a ruptured early endosome with a few AuNPs contained in it and some AuNPs released in the cytosol in close proximity to the endosome. A possible site of membrane rupture is indicated by a white arrow; and, in (c) mitoTGFP conjugated AuNPs (depicted as black spots) are shown making their way into mitochondria. The entry of AuNPs is associated with the rupture of the outer mitochondrial membrane (OMM) as shown by the white arrow. The mitoTGFP conjugated AuNPs are associated with the inner mitochondrial membrane (IMM). Scale bars are 200 nm for a, b and c.

Induction of apoptosis

As the entry of AuNPs into the inner mt membrane partially ruptured the OMM (figures 4 (c)), we hypothesized that the AuNP-mediated rupture of OMM could trigger apoptosis via release of cytochrome *c*, a protein resident in the intermembrane space (IMS).⁴ Cytochrome *c* release could trigger a cascade of caspases, eventually inducing cell death without additional external stimuli. To confirm the apoptotic potential of mitoTGFP-AuNPs, cells transfected with PEG-AuNPs, HAeGFP-AuNPs and mitoTGFP-AuNPs were incubated with a cell-permeable fluorogenic substrate for the apoptotic enzyme caspase 3, which converts the substrate into a fluorescent dye. Caspase activity is a critical step in the onset of apoptosis that can be monitored using this fluorogenic substrate.^{41, 42}

Brightfield images documented healthy cells (figure 5 (a)) with no obvious signs of cell stress (*i.e.* cell shrinkage). Fluorescence images of cells transfected with only the dendrimers PPI-Mal-III G3 as a control (figures 5 (a) – (c)) show almost no fluorescence, documenting the absence of caspase 3 activity (figure 5 (b)). Further, dark spots indicating the presence of nanoparticles were not detectable in brightfield images, as anticipated (figure 5 (a)) confirming previous observations that glycosylated PPI dendrimers are non-cytotoxic.²⁰

Brightfield images further revealed the presence of imported AuNPs (seen as black spots) inside cells transfected with either PEG-AuNPs (figure 5 (d) – (f)), or HAeGFP-AuNPs (figure 5 (g) – (i)) or with mitoTGFP-AuNPs (figure 5 (j) – (l)) in the presence of the cationic PPI glycodendrimer. Although bright-field images of PEG-AuNP or HAeGFP-AuNP transfected cells appeared healthy (figures 5 (d) and 5 (g)), fluorescence images reveal some fluorescent spots (figures 5 (e) and (h)) indicating elevated caspase activity indicative of an early stage of apoptosis.⁴¹

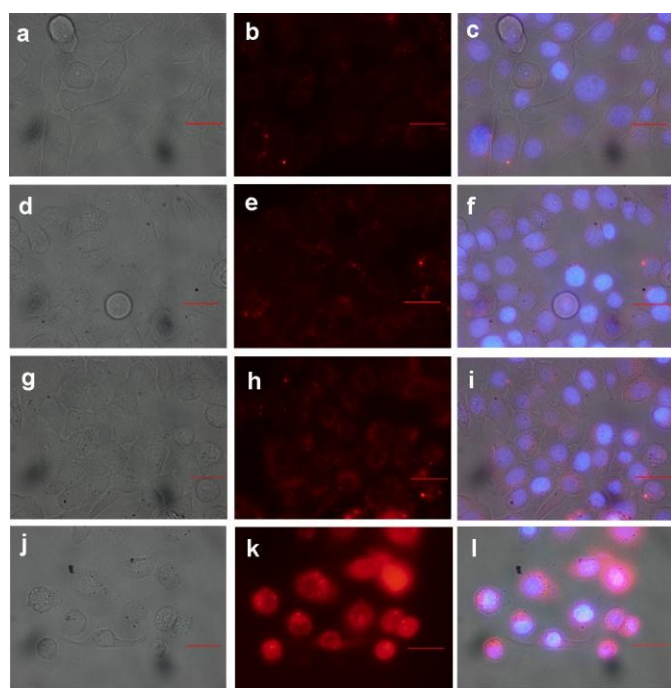
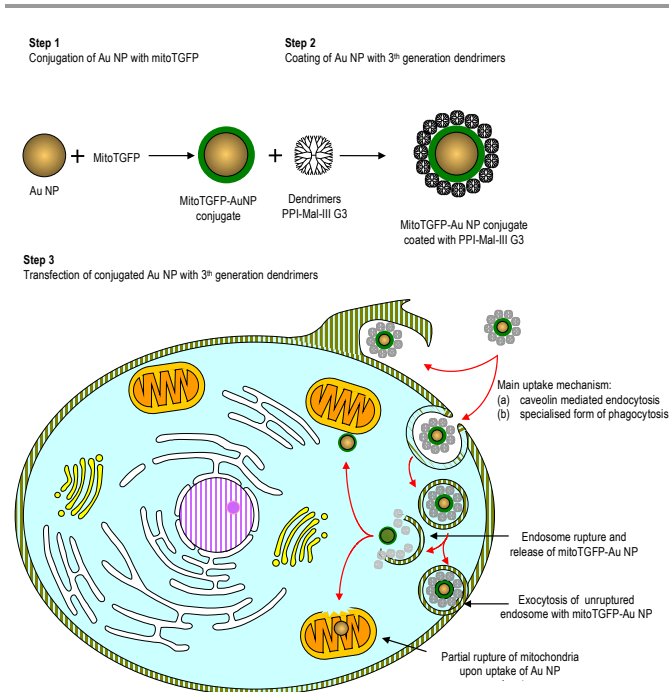


Figure 5. Brightfield and fluorescence images of caspase 3 activity of transfected cells. Cells were transfected with dendrimers only (a-c), PEG-AuNPs (d-f), HAeGFP-AuNPs (g-i) and mitoTGFP-AuNPs (j-l). The figure shows brightfield images (left column), caspase 3 staining (middle column) and overlay images of brightfield, nuclear, and caspase 3 activity staining images (right column). All images were taken under same conditions. The scale bar is 30 μm .

Cells transfected with mitoTGFP-AuNPs possess clear signs of apoptosis including cell shrinkage and rounded cells, clearly observable (figure 5 (j))^{43, 44} with diffuse high intensity fluorescence in the cytoplasm indicating high caspase activity³⁹ and condensed chromatin confirming the progression of cell death (figure 5 (l)).⁴⁵ As seen in TEM images, mitochondria of cells transfected with mitoTGFP-AuNP conjugates experienced outer mitochondria membrane rupture, releasing intermembrane cytochrome *c* to the cytosol, activating a caspase-signalling cascade, leading to programmed cell death.^{4, 46} Cells transfected with purified proteins did not exhibit apoptotic symptoms (See supplementary information – figure S3). Therefore, transfection of mitochondrial localizing AuNP conjugates could be regarded as apoptosis-inducing due to the mechanical disruption of mitochondria, which in turn induces mitochondria-dependent apoptosis. The process is summarised and illustrated in scheme 1.



Scheme 1. Schematic presentation of the procedure in targeting of AuNP to mitochondria as well as illustration of membrane rupture that occurs once the nanoparticle enters the mitochondria.

Experimental

Cell line, cell culture products, chemicals and reagents

Trisodium citrate and tetrachloroauric acid for synthesis of AuNPs were purchased from Sigma Aldrich GmbH, Germany. Synthesis and characterization of the third generation maltotriose modified poly(propylene imine) (PPI) dendrimer (PPI-Mal-III G3) have been described previously.¹⁸ We have used the same charge of PPI-Mal-III G3 as in reference 18. Structure of PPI-Mal-III G3 is presented as supporting information (figure S1). The plasmids encoding the mt localizing turbo green fluorescent protein (mitoTGFP) and green fluorescent protein (GFP) were purchased from Biocat GmbH, Germany. Cloning vectors pet23b+ and *E. coli* strains Top 10F' and BL21 DE3pLys were from Novagen GmbH, restriction enzymes NheI and XhoI were obtained from New England Biolabs GmbH, Germany.

The human cancer line Jimt-1 was obtained from the *Deutsche Sammlung von Mikroorganismen und Zellkulturen* (DSMZ) GmbH, Germany. The cell line, derived from the pleural effusion of a 62-year-old woman with ductal breast cancer after postoperative radiation in 2003, was reported to carry an amplified HER-2 oncogene and to be insensitive to HER-2-inhibiting drugs such as trastuzumab (Herceptin).^{47, 48} Media and reagents for cell culture including Dulbeccos Modified Eagles Medium (DMEM) without phenol red, phosphate-buffered saline, trypsin, and penicillin/streptomycin were from PAA Laboratories GmbH, Germany. Microcell culture dishes (35 mm diameter) for transfection were purchased from Ibidi GmbH, Martinsried, Germany. The caspase 3 substrate

Phiphilux-G2D2 is a product of Oncoimmun Inc. and was obtained from EMD Millipore, Germany.

Fixation, staining and resin embedding reagents for Transmission Electron Microscopy (TEM) sample preparation including glutaraldehyde, low melting agarose, uranyl acetate, osmium tetroxide, lead citrate, modified Spurr embedding kit were purchased from Serva Electrophoresis GmbH, Germany, copper grids from Plano GmbH, Germany.

Gold nanoparticles

Spherical AuNPs were prepared by citrate reduction according to Frens et al.²⁵ For the preparation of AuNPs with 20 nm diameter, 2.5 ml of 1% trisodium citrate solution were added to 10 ml 0.1% tetrachloroauric acid ($\text{HAuCl}_4 \cdot 3\text{H}_2\text{O}$). The mixture was stirred for 30 min at 70 °C until the colour changed from colourless to ruby red. The resulting AuNPs were characterized by UV Vis spectrophotometer (Varian Cary 100, Canterbury, Australia) and SEM-EDX (Leo 982 scanning electron microscope, Carl Zeiss GmbH, Germany) (see supplementary information – figure S2). Formation of AuNP can also be quantitatively verified at elemental level using XRD.

Expression of fluorescent proteins

The AuNPs used in the experiments were conjugated to mitoTGFP or HAeGFP (haemagglutinin-tagged green fluorescent protein). The genes encoding mitoTGFP and HAeGFP were cloned, expressed and the respective proteins were purified. MitoTGFP was amplified by Polymerase Chain Reaction (PCR) from a plasmid bearing the mitoTGFP gene using gene specific primers with additional NheI/XhoI restriction sites. Upon treatment with the respective enzymes the PCR product was cloned into the pET23b+ vector with an inherent histidine tag and transformed into competent cells of *Escherichia coli* strain TOP10F⁷. Plasmids isolated from positive clones were confirmed by DNA sequencing and transformed into *Escherichia coli* strain BL21 (DE3) pLysS for expression of mitoTGFP. Transformants were grown at 30 °C in LB medium with ampicillin and chloramphenicol to an absorbance OD600 of 0.5 followed by a 4 hour induction with 0.5 mM IPTG. MitoTGFP was purified under native conditions using nickel beads as previously described.²⁴ To check the mt targeting specificity of mitoTGFP, an eGFP variant containing the viral haemagglutinin tag instead of the mt targeting signal at its N terminus was cloned, expressed and purified using the same procedure.

Conjugation of AuNPs to proteins

The concentration of AuNP was calculated by Beers law using the known molar extinction coefficient of 20 nm AuNP in water ($1.6 \text{ M}^{-1} \text{ cm}^{-1}$)²⁵ with AuNP solution optical density measured by UV-Vis-spectroscopy. To conjugate AuNPs to mitoTGFP, 100 μl of 0.1 nM AuNPs (20 nm diameter) were incubated with 100 μl of mitoTGFP (0.05 $\mu\text{g}/\mu\text{l}$ in PBS pH 5.5) for 15 min in the dark at room temperature. After incubation, the samples were centrifuged at 7000 g for 15 min. The resulting conjugates were re-suspended in 100 μl PBS (pH 7.4). Conjugation of

AuNPs (0.1 nM) with HAeGFP was conducted in an identical manner. To conjugate AuNPs to polyethylene glycol, 100 μl AuNPs (0.1 nM) were mixed with 100 μl 20% (w/v) freshly prepared polyethylene glycol (PEG) 3350 dissolved in water and incubated as per the protein-AuNP conjugates with 100 μl of the conjugates pipetted into 96-well plates. The localized surface Plasmon resonance (LSPR) shift in the absorbance spectrum was used to analyse AuNP conjugates with confirmation by electrophoretic migration of 40 μl of AuNP conjugate suspension in 0.5 % agarose gel at 10 KV per cm in TBE buffer (Tris-Borate-Ethylenediamine Tetraacetic Acid (EDTA)) at pH 8.0.

Transfection and targeting AuNPs to mitochondria

Jimt-1 cells were grown in DMEM with 4,500 g/l glucose, 10% (v/v) fetal calf serum and 2 mM l-glutamine (PAA Laboratories GmbH) without phenol red at 37 °C and 5 % CO₂. Cells were routinely sub-cultured three times a week by enzymatic detachment using trypsin.

For apoptosis assays, 3 x 10⁵ cells were seeded in 35 mm microcell culture dishes one day before transfection. Transfection complexes with mitoTGFP-AuNPs were constituted by adding 100 μl of AuNP-protein conjugate suspension to 100 μl HEPES buffer (pH 7.4). To this mixture, 100 μg of PPI-Mal-III G3 were added and mixed thoroughly. Transfection complex mixtures were incubated for 15 min at room temperature before being transferred to the cell suspension. After incubation for 4 h at 37 °C and 5% CO₂ in the absence of serum, transfection was stopped by washing the cells twice with PBS. Thereafter, the incubation was continued for a further 24 h with serum to allow targeting of AuNP conjugates to mitochondria. Control treatments included mock transfection (incubation with PPI-Mal-III G3 only) and non-transfected cells to assess autofluorescence. Cells were analysed using fluorescence and transmission electron microscopy to verify the efficacy of PPI-Mal-III G3 as a transfection reagent. To verify apoptosis, transfected cells were incubated with 200 μl PhiphiluxG2D2 for 1 h followed by washing with 2 ml PBS.^{26, 27}

Validation of mitochondrial targeted AuNPs

Transmission Electron Microscopy (TEM) was used to assess if AuNPs successfully targeted mitochondria. For TEM investigations, 1 x 10⁶ Jimt-1 cells were grown in 100 mm sterile Petri dishes. After transfection, the cells were detached using trypsin and fixed with 2.5 % glutaraldehyde in DMEM buffer at 37 °C and 5% CO₂ for 24 h. The samples were then encapsulated in 2% low melting agarose gel for 30 min at 4 °C. The gel-encapsulated cells were sliced (about 1.5 x 1 mm) and fixed with 1% osmium tetroxide for 24 h then washed three times for 15 min with distilled water. A series of 25%, 50%, 75%, 96% and 100% acetone/water mixtures (v/v) were used to dehydrate samples over 4 h and then stained by 1% uranylacetate in acetone. The gel slices were stepwise embedded in epoxy resin in (30% for 4 h; 50% for 12 h; 70% for 4 h; 100% for 4 h; 100% for 12 h; and, lastly 100% for 4 h.

The resin was stepwise polymerized at 50 °C for 3 h, then 55 °C - 60 °C over 72 h.²⁸ Ultra-thin sections (50 nm) were prepared on a Lexica Electron M Ultracut ultramicrotome, mounted on pioloform-coated copper grids and post-stained with uranylacetate and lead citrate.²⁹ Electron micrographs were taken with a Scanning TEM at 30 kV or Zeiss 912 Omega (Carl Zeiss GmbH, Germany) at 120 kV. Further, verification cellular uptake can be done with complementary ICP-MS analysis. The mitochondria should be extracted from the whole cancer cells and then measure the amount of Au by ICP-MS.

Apoptosis verification

To confirm the apoptotic potential of mitoTGFP-AuNPs, cells transfected with PEG-AuNPs, HAeGFP-AuNPs and mitoTGFP-AuNPs were incubated with a cell-permeable fluorogenic substrate for the apoptotic enzyme caspase 3, which converts the substrate into a fluorescent dye. The CaspGLOW™ Fluorescein Active Caspase-3 Staining Kit was used and the cells were observed under a fluorescence microscope using FITC filter. Caspase positive cells appeared to have brighter green signals, whereas caspase negative control cells show much weaker signal.

Conclusions

In this work, we successfully transfected AuNP conjugates inside cells using cationic PPI glycodendrimer with open maltotriose shells with targeting of AuNPs conjugated to mitoTGFP. Further, the entry of AuNPs into mitochondria ruptured the outer mitochondrial membrane, triggering apoptosis. Transfection of mitochondrial localizing AuNP conjugates induces apoptosis due to the mechanical disruption of mitochondria, which in turn induces mitochondria-dependent apoptosis. This study provides a step towards development of controlled and targeted induction of apoptosis in cancer cells, which could provide an important tool in cancer therapy.

Acknowledgements

We thank Kai Ostermann (TU Dresden, Institute of Genetics) and Jörg Opitz (Fraunhofer Institute of Non-destructive Testing) for helpful comments on the manuscript, Hartmut Komber (Leibniz-Institut für Polymerforschung Dresden e.V.) for NMR experiments, Nora Haufe (TU Dresden, Institute for Physical Chemistry) for assistance with the ultra-microtome and Axel Mensch (TU Dresden, Institute of Materials Science) for support in TEM. This work was partially funded by the BMBF Competence Centre 'Ultradünne funktionale Schichten' Dresden, and the joint BMBF-funded project (Nr. 13140845) of the Friedrich-Schiller Universität Jena and the Technische Universität Dresden in conjunction with the DFG research training group "Nano- und Biotechniken für das Packaging elektronischer Systeme" (DFG 140/1), Germany. Finalization of the work has been made possible through support funds from the Enterprise Cape Breton Corporation (ECBC) to the

Industrial Research Chair for Mine Water Management at Cape Breton University, Nova Scotia, Canada.

Notes and references

^a Encyt Technologies Inc., 201 Churchill Drive, Membertou, NS, Canada B1S 0H1

^b Technische Universität Dresden, Institute of Genetics, 01062 Dresden, Germany

^c Technische Universität Dresden, Institute of Materials Science and Max Bergmann Centre for Biomaterials, 01062 Dresden, Germany

^d Leibniz-Institut für Polymerforschung Dresden e.V., Hohe Straße 6, 01069 Dresden, Germany

^e Verschuren Centre for Sustainability in Energy and the Environment, Cape Breton University, 1250 Grand Lake Road, Sydney, Nova Scotia, Canada B1P 6L2.

† Electronic Supplementary Information (ESI) available: [PPI-Mal-III G3 Dendrimers; SEM of AuNP and TEM of AuNP interaction with cancerous cells; and comparison of brightfield and caspase 3 fluorescence staining verifying apoptosis].

1. D.-F. Suen, K. L. Norris and R. J. Youle, *Genes & Development*, 2008, **22**, 1577-1590.
2. D. R. McIlwain, T. Berger and T. W. Mak, *Cold Spring Harbor Perspectives in Biology*, 2013.
3. L. Galluzzi, N. Larochette, N. Zamzami and G. Kroemer, *Oncogene*, 2006, **25**, 4812-4830.
4. S. Biswas and V. P. Torchilin, *Advanced drug delivery reviews*, 2014, **0**, 26-41.
5. I. H. El-Sayed, X. Huang and M. A. El-Sayed, *Cancer Letters*, 2006, **239**, 129-135.
6. V. P. Zharov, E. N. Galitovskaya, C. Johnson and T. Kelly, *Lasers in Surgery and Medicine*, 2005, **37**, 219-226.
7. K. Sokolov, M. Follen, J. Aaron, I. Pavlova, A. Malpica, R. Lotan and R. Richards-Kortum, *Cancer Research*, 2003, **63**, 1999-2004.
8. X. Zhang, H. Chibli, R. Mielke and J. Nadeau, *Bioconjugate Chemistry*, 2011, **22**, 235-243.
9. P. K. Jain, X. Huang, I. H. El-Sayed and M. A. El-Sayed, *Accounts of Chemical Research*, 2008, **41**, 1578-1586.
10. P. K. Jain, K. S. Lee, I. H. El-Sayed and M. A. El-Sayed, *Journal of Physical Chemistry B*, 2006, **110**, 7238-7248.
11. X. Huang, I. H. El-Sayed, W. Qian and M. A. El-Sayed, *NANO LETTERS*, 2007, **7**, 1591-1597.
12. J. Kneipp, H. Kneipp, M. McLaughlin, D. Brown and K. Kneipp, *Nanoletters*, 2006, **6**, 2225-2231.
13. S. Grosse, Y. Aron, I. Honore, G. Thevenot, C. Danel, A.-C. Roche, M. Monsigny and I. Fajac, *The Journal of Gene Medicine*, 2004, **6**, 345-356.
14. H. Arima, Y. Chihara, M. Arizono, S. Yamashita, K. Wada, F. Hirayama and K. Uekama, *Journal of Controlled Release*, 2006, **116**, 64-74.
15. S. S. Diebold, M. Kurs, E. Wagner, M. Cotten and M. Zenke, *The Journal of Biological Chemistry*, 1999, **274**, 19087-19094.

16. R. Haag and F. Kratz, *Angewandte Chemie International Edition*, 2006, **45**, 1198-1215.
17. M. Mkandawire, A. Pohl, T. Gubarevich, V. Lapina, D. Appelhans, G. Rödel, W. Pompe, J. Schreiber and J. Opitz, 2, 2009, **10**, 596-606.
18. T. Pietsch, D. Appelhans, N. Gindy, B. Voit and A. Fahmi, *Colloids and Surfaces A: Physicochemical and Engineering Aspects*, 2009, **341**, 93-102.
19. M. Kubeil, H. Stephan, H.-J. Pietsch, G. Geipel, D. Appelhans, B. Voit, J. Hoffmann, B. Brutschy, Y. V. Mironov, K. A. Brylev and V. E. Fedorov, *Chemistry – An Asian Journal*, 2010, **5**, 2507-2514.
20. B. Klajnert, D. Appelhans, H. Komber, N. Morgner, S. Schwarz, S. Richter, B. Brutschy, M. Ionov, A. K. Tonkikh, M. Bryszewska and B. Voit, *Chemistry - A European Journal*, 2008, **14**, 7030 - 7041.
21. M. Fischer, D. Appelhans, B. Klajnert, M. Bryszewska, B. Voit and M. Rogers, *Biomacromolecules*, 2010, **11**, 1314-1325.
22. B. Ziemia, A. Janaszewska, K. Ciepluch, M. Krotewicz, W. A. Fogel, D. Appelhans, B. Voit, M. Bryszewska and B. Klajnert, *Journal of Biomedical Materials Research Part A*, 2011, n/a-n/a.
23. K. Rennstamm, G. Jönsson, M. Tanner, P. Bendahl, J. Staaf, A. I. Kapanen, R. Karhud, B. Baldetorp, A. Borg and J. Isola, *Cancer Genetics and Cytogenetics*, 2007, **172**, 95-106.
24. L. Wang, Y. Liu, W. Li, X. Jiang, Y. Ji, X. Wu, L. Xu, Y. Qiu, K. Zhao, T. Wei, Y. Li, Y. Zhao and C. Chen, *Nano Letters*, 2011, **11**, 772-780.
25. G. Frens, *Nature Physical Science*, 1973, **241**, 20-22.
26. W. D. Geoghegan and G. A. Ackerman, *The Journal of Histochemistry and Cytochemistry*, 1977, **25**, 1187-1200.
27. A. Gole, C. Dash, C. Soman, S. R. Sainkar, M. Rao and M. Sastry, *Bioconjugate Chemistry*, 2001, **12**, 684-690.
28. R. T. Tom, A. K. Samal, T. S. Sreepasad and T. Pradee, *Langmuir*, 2007, **23**, 1320-1325.
29. M.-E. Aubin, D. G. Morales and K. Hamad-Schifferli, *NanoLetters*, 2005, **5**, 519-522.
30. S. Häbel, A. Loos, D. Appelhans, S. Schwarz, J. Seidel, B. Voit and A. Aigner, *Journal of Controlled Release* 2011, **149**, 146-158.
31. C. Brandenberger, C. Mühlfeld, Z. Ali, A.-G. Lenz, O. Schmid, W. J. Parak, P. Gehr and B. Rothen-Rutishauser, *Small*, 2010, **6**, 1669-1678.
32. C. Tekle, B. v. Deurs, K. Sandvig and T.-G. Iversen, 2008, **8**.
33. B. D. Chithrani, James Stewart, C. Allen and D. A. Jaffray, *Nanomedicine: Nanotechnology, Biology, and Medicine* 2009, **5**, 118 -127.
34. A. M. Derfus, W. C. W. Chan and S. N. Bhatia, *Advanced Materials*, 2004, **16**, 961-966.
35. P. Nativo, I. A. Prior and M. Brust, *ACS Nano*, 2008, **2** 1639-1644.
36. G. J. Doherty and H. T. McMahon, *Annual Review of Biochemistry*, 2009, **78**, 857-902.
37. T. Komiya and K. Mihara, *Journal of Biological Chemistry*, 1996, **271**, 22105-22110.
38. W. P. Sheffield, G. C. Shore and S. K. Randall, *Journal of Biological Chemistry*, 1990, **265**, 11069-11076.
39. N. Wiedemann, A. E. Frazier and N. Pfanner, *The Journal of Biological Chemistry*, 2004, **279**, 14473-14476.
40. N. Pfanner and A. Chacinska, *Biochimica et Biophysica Acta*, 2002, **1592**, 15- 24.
41. W. G. Telford, A. Komoriya and B. Z. Packard, *Cytometry Part A*, 2002, **47**, 81-88
42. A. Komoriya, B. Z. Packard, M. J. Brown, M.-L. Wu and P. A. Henkart, *The Journal of Experimental Medicine*, 2000, **191**, 1819-1828.
43. X. Jiang and X. Wang, *Annual Reviews in Biochemistry*, 2004, **73**, 87-106.
44. J. F. Kerr, A. H. Wyllie and A. R. Currie, *British Journal of Cancer*, 1972, **26**, 239-257.
45. M. R. Alison and C. E. Sarraf, *Human and Experimental Toxicology*, 1995, **14**, 234-247.
46. V. Borutaite, *Environmental and Molecular Mutagenesis*, 2010, **51**, 406-416.
47. V. Roy and E. A. Perez, *The Oncologist*, 2009, **14**, 1061-1069.
48. J. C. Singh, K. Jhaveri and F. J. Esteva, *Br J Cancer*, 2014, **111**, 1888-1898.